ISSN 1330-3651 (Print), ISSN 1848-6339 (Online)
https://doi.org/10.17559/TV-20211026210931
Original scientific paper

Determination of the Change in Electrical Conductivity of Single, Bimetallic and Trimetallic Cylindrical Billets with Plastic Deformation Induced by Upsetting Process

Isik CETINTAV, Cenk MISIRLI*, Yilmaz CAN

Abstract: In this study, measurement of the effect of singular, bimetallic and multimetallic materials exposed to cold plastic deformation on electrical conductivity properties was investigated. The main subject of this research is plastic deformation occurring in the upsetting process and changing the conductivity properties of the parts. In the experiments, steel, aluminium, copper, brass, bimetallic and multimetallic materials designed with different combinations of these materials were used as test materials. Experimental upsetting tests were performed as a height reduction ratio 10%, 20% and 30%. The electrical conductivity measurement results of the deformed samples were obtained with a conductivity measuring device. The results obtained from the experiments are presented in graphs with electrical conductivity axis that change due to deformation. As a result of the experiments and measurements, it was concluded that the electrical conductivity of the deformed materials generally decreased slightly due to the plastic deformation of the deformed materials, and the bimetallic and multimetallic materials were similar to the properties of the majority material.

Keywords: aluminium; bimetallic; brass; conductivity; copper; deformation; electrical; steel; trimetallic

1 INTRODUCTION

Bimetallic and Trimetallic materials are composite-like materials that are formed by physically combining two or more materials with different properties. The purpose of this combination is to take advantage of the superior properties of the combined materials themselves and to ensure that the new material has superior properties. The most commonly used materials in the production of bimetallic and trimetallic materials are copper, aluminium, brass and steel. Copper, aluminium and brass have high electrical and thermal conductivity, making them essential materials for electrical conduction and heat transfer engineering. Due to the decrease in copper mines, it has become inevitable to use aluminium instead of copper. Compared to copper, aluminium has poor welding performance, greater surface contact resistance, so it is still difficult to use aluminium instead of copper to make many pieces directly. For example, the product of copper-aluminium coating sheet covering a copper layer on the surface of the aluminium plate can increase the surface contact resistance and welding properties of aluminium, which reduces the cost and weight. Many important parts of electrical equipment such as heat exchanger, electrical conduction and cooling fins, collector pipes, transition plates are normally made of copper-aluminium coated metals. Likewise, copper-clad aluminium conductor wire is also a good application of metal-clad metals in the electrical, electronics industry. Copper clad aluminium conductive wire overcomes the problems of contact and creep of pure aluminium wires. Compared to pure copper wires, it can reduce expensive copper consumption. Other examples of electrical conductivity applications of bimetallic and trimetallic materials in the industry; copper-aluminium coated metals; transformer belts; solar panels, etc. copper-aluminium clad terminals, copper-aluminium clad transition plates, copper-aluminium clad clamps, copper-aluminium clad seals, etc. copper-aluminium coated transition joints, copper-aluminium coated conductor rods; copper-aluminium coated electrodes; copper-aluminium coated conductor sleeves for the electrolysis unit, etc. Bimetallic and Trimetallic materials are also used as bearing materials. Advantages as a bearing material: high load carrying capacity, low friction, long service life, low vibration, etc.

A material whose properties depend on the lattice structure is affected by plastic deformation or cold forming processes. Cold forming can be described as deforming a material below the recrystallization temperature. In other words, the process of changing the shape or cross-section of a metal at a temperature below the softening or recrystallization point, usually around room temperature. Examples of these operations include drawing, rolling, forging and stretching. As a result of the process, while the ductility of the material decreases, the tensile strength, yield strength and hardness increase. Stiffness increases during cold deformation due to strain hardening [1]. Due to the cold forming or deformation process, the lattice structure is distorted, this prevents the passage of electrons and reduces the electrical conductivity. Some studies showed that electrical conductivity of aluminium, copper and brass decreases slightly due to plastic deformation in the deformed materials [2]. This effect is mild in pure metals but remarkable in alloys [3]. Cold forming or deformation is a powerful method with a slightly undesirable effect on electrical conductivity [4]. In general, materials with high strength have low electrical conductivity. In other words, strength and electrical conductivity are opposite [5].

Many studies have been conducted on the electrical conductivity of copper, aluminium, brass and steels, which are a copper alloy. Estrin et al. [6] demonstrated an increase in material strength without loss of electrical conductivity for a particular bar geometry out of three geometries tested by equal channel angular pressing at 175 °C. Wei et al. [7] investigated the microstructure, mechanical properties and electrical conductivity of Cu-0,5% Cr, an alloy commonly used in industry, as a result of equal channel angular pressing (ECAP) and cold rolling with and without aging process.

2 EXPERIMENTAL WORK

2.1 Upsetting Tests

To examine the interaction between different metals, four models were designed in this study. The material

combinations and properties of these models are shown in Tab. 1.

Table 1 Material Combinations

AISI 1020 STEEL

C / %	Mn / %	P / %	S / %	Fe / %
0,2	0,5	0,05	0,05	Rest

COPPER

O / %	Cu / %
0,04	99,9

ALUMINUM 5083

Fe / %	Si / %	Cu / %	Mg / %	Mn / %	Al / %
0,09	0,05	0,005	4,5	1	rest

BRASS

Pb / %	Al / %	Fe / %	Ni / %	Sn / %	Cu / %	Zn / %
1,6	0,05	0,3	0,3	0,3	62	rest

Figure 1 Some examples of multi-metallic material models [1]

The final version of the basic designs of these four models is shown in Fig. 1. After all metals are prepared in appropriate dimensions on the lathe machine, the first step for bimetallic materials is the first inner solid cylinder (copper and brass) pressed into the outer ring material (steel) with low pressure. For trimetallic materials the inner solid cylinder (aluminium) is the outer ring with low pressure. It is pressed into the material (copper and brass) and then pressed into the outer ring material (steel). These pieces are called bimetallic and trimetallic materials. The resulting multimetallic components and models are shown in Fig. 2. In addition, single metal cylindrical billets forming multimetallic parts are shown in Fig. 3. This value was converted to a resistance value, then this resistance value, thus the pressure value, was provided to the software as input value.

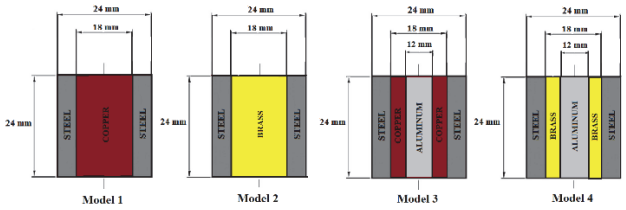

Figure 2 Design of multi-metallic material models

Fig. 3 also shows a 60-ton hydraulic press with a constant speed of 0,1 mm/s where experiments were carried out. The hydraulic press is equipped with a pressure-current transducer to measure the upsetting load and save it to the computer. The load or pressure value can be read by an I/O card of the personal computer during the upsetting experiment.

Before the experiments, samples and flat molds were oiled, sanded and cleaned with alcohol using a special lubricant named MoS2 [8-10]. Fixing the system to the hydraulic press just before the test is shown in Fig. 4. Cylindrical billets are forged in open die at 10%, 20% and 30% height reduction rates.

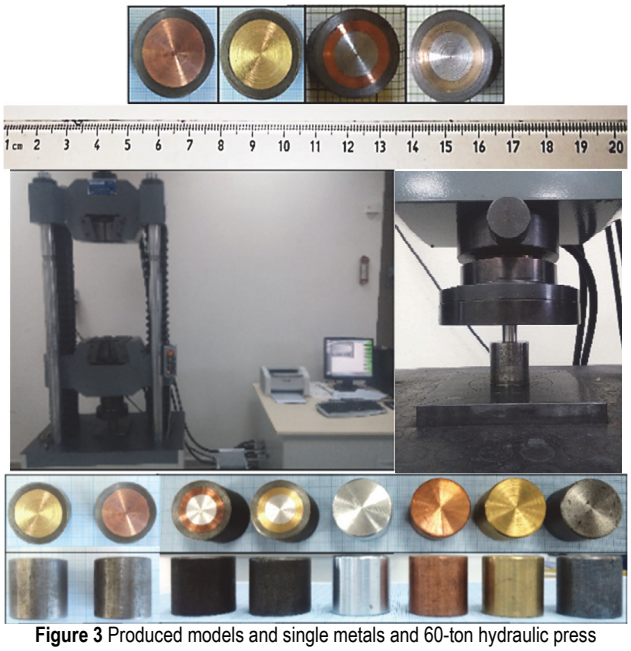

Figure 3 Produced models and single metals and 60-ton hydraulic press

After the upsetting process, the samples were cut along the *x-z* plane and the barrel profiles and interface conditions of the inner solid cylinder, middle ring and outer ring were examined. Fig. 4 shows the deformation and barrelling of bimetallic and trimetallic parts after 30% height reduction. Fig. 6 shows the conditions of the materials after 10%, 20% and 30% height reduction. In general, it has been observed that all models have material flow as desired. Some models have small gaps between layers after 30% reduction. It has been observed that the interior materials especially the meridian cross section flow very rapidly and a barrel profile is different from a normal barrel spring [10-12]. Since the outer materials generally trap the inner cylindrical metal, especially the interfaces close to the die cannot move easily. Inner cylinder material barrel profile is not the same as outer ring material barrel profiles.

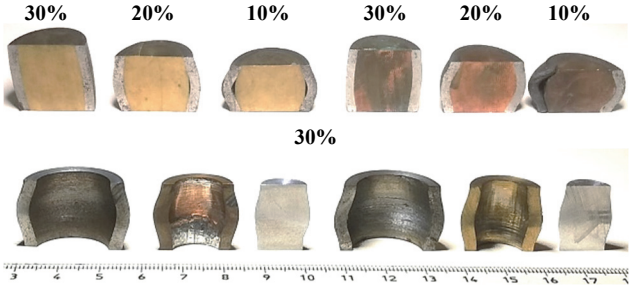

Figure 4 Deformations, barreling and cavities after 10%, 20% and 30% height reduction

In Model 1, it is also seen that there is no contact between the inner and outer metal and that there is a gap in the middle of the inner material, namely in the meridian part. This gap can be explained in the following way: inhomogeneous deformation occurs in the center line and this gap is attributed to a hydrostatic stress state. The experimental results obtained showed that the metal flow was not homogeneous for these four models, especially for

solid cylinder materials. Outer rings and shear of solid roll materials also affect metal flow and load requirement.

2.2 Measurement of Electrical Conductivity

The measure of a material's ability to conduct electrical current is called electrical conductivity. At the same time, electrical conductivity is the opposite of electrical resistance, which measures the ability to resist electric current. Electrical conductivity in metals is established using Ohm's Law, which explains that the current flowing through a conductor between any two points on the metal is directly proportional to the potential difference between these two points. The electrical resistance of the material, which is constant for each material and accepted as a property, allows the classical mathematical equation to be correct for this connection.

The electrical conductivity of the same cylindrical billets with 24 mm height and 24 mm diameter was measured with an accuracy ±2 in % IACS using SIGMACHECK 2 EDDY CURRENT CONDUCTIVITY METER, an electrical conductivity measurement device. The unit of electrical conductivity is Siemens per meter in the SI unit system, but devices conductivity usually express values in % IACS units. The % IACS value is obtained by multiplying the conductivity values in Siemens / meter by $1{,}7241\times10^{-6}$. Electrical conductivity devices work according to the eddy current method. Since the size and shape of the samples tested can affect the measurement, all samples tested were chosen to have the same geometry.

Electromagnetic induction is the basis of eddy current technology. Maxwell's Ampere law proves that when alternating current is passed through a wire, it creates a magnetic field, also called the primary magnetic field that depends on time. Electromagnetic induction occurs when a conductor gets close to a time-varying magnetic field. This situation causes the induction of electrical voltage inside the conductor. The current generated is induced along planes perpendicular to the magnetic induction vector and generates eddy currents (the name is so called because its shape resembles a vortex). Eddy current probes have an element on a coil that creates an alternating current, and this coil creates an alternating magnetic field that causes eddy currents in the material to be measured. In this way, the counter magnetic field resisting the magnetic field generated on the coil is created by eddy currents as in Fig. 5 [13].

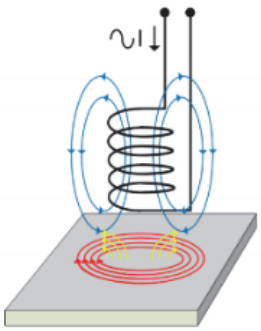

Figure 5 Basis of eddy current theory [13]

The interaction of the magnetic fields generated is related to the distance between the coil and the material to be measured and the actual material composition. If the distance between the material and the coil changes, through the same coil or another sensing coil, the electronic measuring system detects the change in field interaction and produces a voltage output due to the change in the distance between the probe and the target [13]. To make it possible to distinguish between different materials, there is also a change in the field interaction that produces a change in voltage output when the material target is different. Eddy currents are explained according to Ampere, and Faraday laws. Ampere's law Eq.(1) is defined as generalizing to any closed random shape involving many magnetic field lines, Faraday's law Eq. (3) explains that a changing magnetic flux will induce a non-electrostatic electric field that can change with time.

$$\oint_S \vec{B}\mathrm{d}\vec{s} = \mu_0 I \tag{1}$$

where I is the electric current flowing through the surface bounded by the closed path and μ_0 is the permeability of the free space. Given a long radius r wire, the magnetic field B carrying a current I with uniform current density is given by:

$$B = \frac{\mu_0 I}{2\pi r} \tag{2}$$

Faraday's law states that a magnetic flux from one state to another will induce a non-electrostatic electric field that can change over time.

$$\oint_S \vec{E}\mathrm{d}\vec{s} = -\frac{\mathrm{d}\Phi_B}{\mathrm{d}t} \tag{3}$$

where

$$\Phi_B = \int \vec{B}\mathrm{d}\vec{A} \tag{4}$$

The law that states that it produces magnetic fields that tend to oppose the change in magnetic flux that induces such currents is called Lenz's law and the relationship between Electromotive Force (EMF);

$$\varepsilon = -\frac{\mathrm{d}\Phi_B}{\mathrm{d}t} \tag{5}$$

The magnetic field B produced by the probe containing a coil on the material to be measured for electrical conductivity generates an electrostatic current on a conductive material. This electrostatic current creates an opposite magnetic field from the original that affects the coil impedance. Material cavities and different material conductivity affect the induced currents and the counter magnetic field, so the coil impedance also changes. This allows to characterize or detect different conductive materials.

As shown in Fig. 6, with the help of the impedance diagram, it is possible to interpret the eddy currents data. This diagram includes the variation of the strength of eddy

currents and the magnetic permeability of the material. In materials with different conductivities, the eddy current signal reacts differently in the impedance diagram.

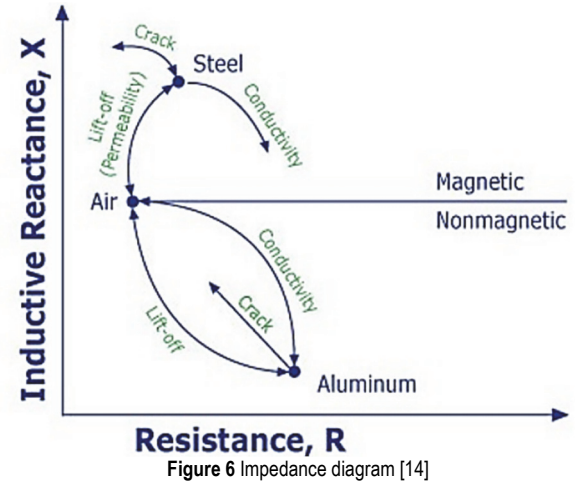

Figure 6 Impedance diagram [14]

3 RESULTS

In this study, upsetting tests of composite-like bimetallic and trimetallic materials produced by using different materials were performed and the electrical conductivity corresponding to certain reductions was measured and the deformation amount and changes in electrical conductivity values were determined.

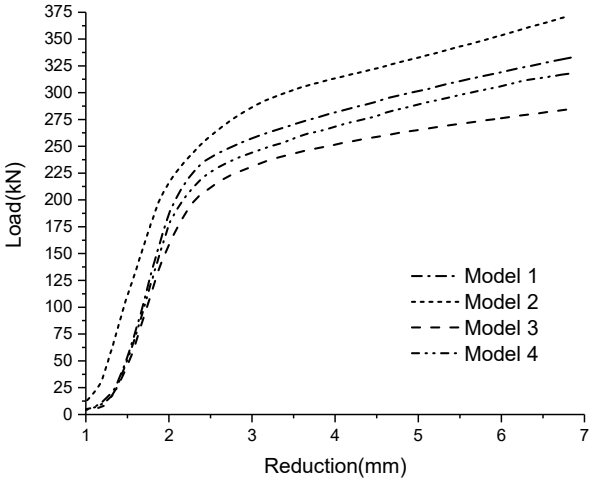

Figure 7 Experimental load-reduction curves for the models

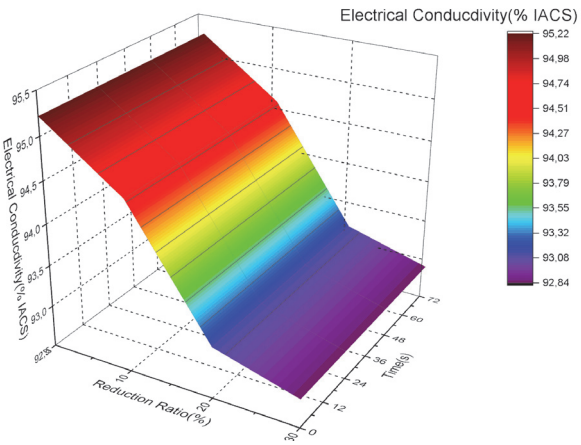

Figure 8 Single copper billet electrical conductivity change after 0, 10%, 20%, 30% reduction

In Figs. 8, 9, 10 and 11, changes in electrical conductivity of copper, aluminum, brass and steel single cylindrical billets after 0, 10%, 20% and 30% deformation are graphically displayed. As seen in Fig. 8, copper billet has the highest electrical conductivity with 95,3% IACS and after 10% deformation, the electrical conductivity value decreases to 94,1% IACS value. When the 30% deformation rate is reached, the electrical conductivity value becomes 92,84% IACS. For the hydraulic press with 0,1 mm/s advance speed, the total time value corresponding to 30% deformation is 72 seconds.

Also seen in Figs. 9, 10 and 11, aluminum, brass and steel billet has electrical conductivities with 33,35%, 24,62% and 10,64% IACS and after 10% deformation, the electrical conductivity values decrease to 32,80%, 24,26%, 10,46% IACS values, finally when the 30% deformation rate is reached, the electrical conductivity values become 30,60%, 22,83%, 8,93% IACS, respectively. For the hydraulic press with 0,1 mm / s advance speed, the total time value corresponding to 30% deformation is 72 seconds. The data obtained show that the losses in electrical conductivity after deformation in single copper, aluminum, brass and steel cylindrical billets were 0,025%, 0,0825%, 0,0725% and 0,175%, respectively. It has been observed that the losses are lower in materials with high electrical conductivity values.

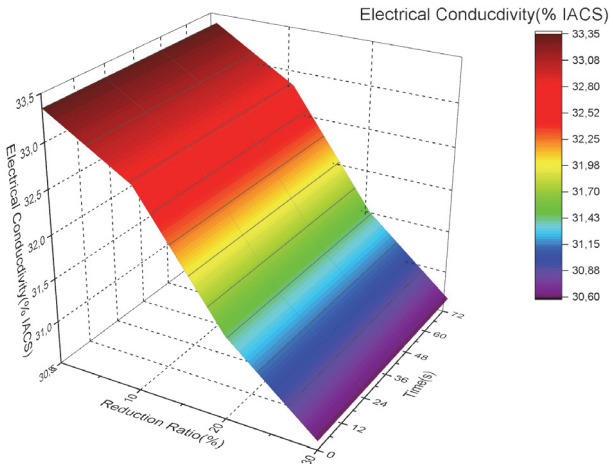

Figure 9 Single aluminum billet electrical conductivity change after 0, 10%, 20%, 30% reduction

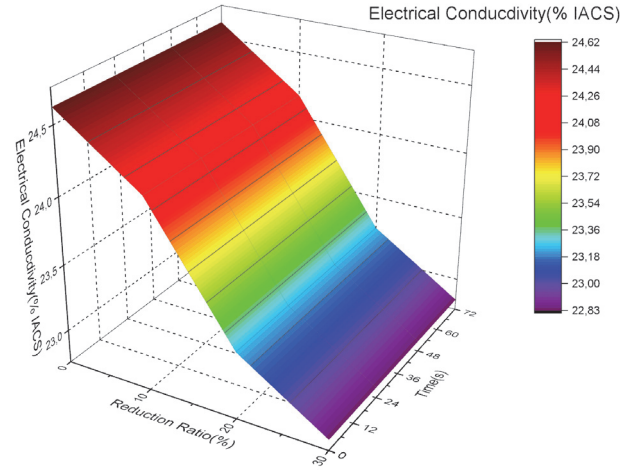

Figure 10 Single brass electrical conductivity change after 0, 10%, 20%, 30% reduction

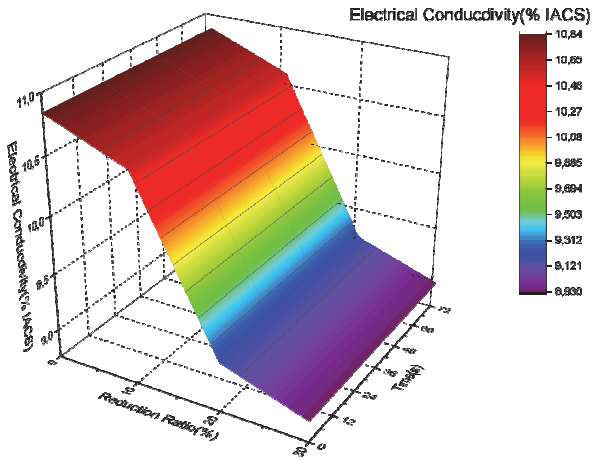

Figure 11 Single steel billet electrical conductivity change after 0, 10%, 20%, 30% reduction

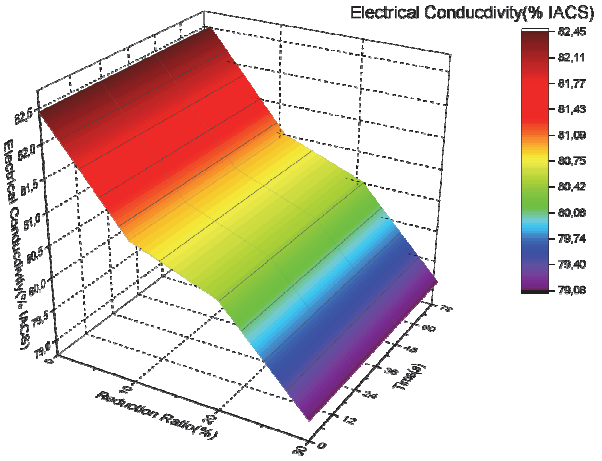

Figure 12 Model 1 billet electrical conductivity change after 0, 10%, 20%, 30% reduction

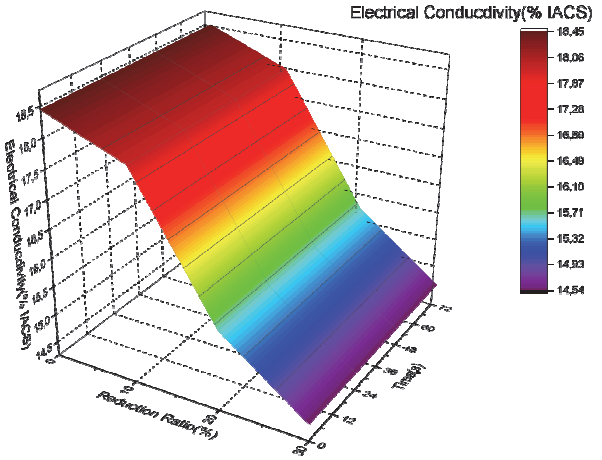

Figure 13 Model 2 billet electrical conductivity change after 0, 10%, 20%, 30% reduction

In Fig. 12 and Fig. 13, the electrical conductivity-deformation-time graphs of the Model 1 and Model 2 bimetallic cylindrical parts are shown. As can be remembered from single cylindrical billets, copper is the material with the highest electrical conductivity. For this reason, Model 1, which contains copper, has a very high electrical conductivity. As Model 2 is a brass-containing model, its electrical conductivity is very low. Model 1 and Model 2 have 82,45% IACS and 18,45% IACS electrical conductivity, respectively, for 0% deformation amount, that is, before the upsetting process starts. After 30% deformation, these electrical conductivity values decrease to 79,06% and 14,54%, respectively. The loss rate in electrical conductivity after upsetting for Model 1 is 0,05%, for Model 2 it is around 0,2%.

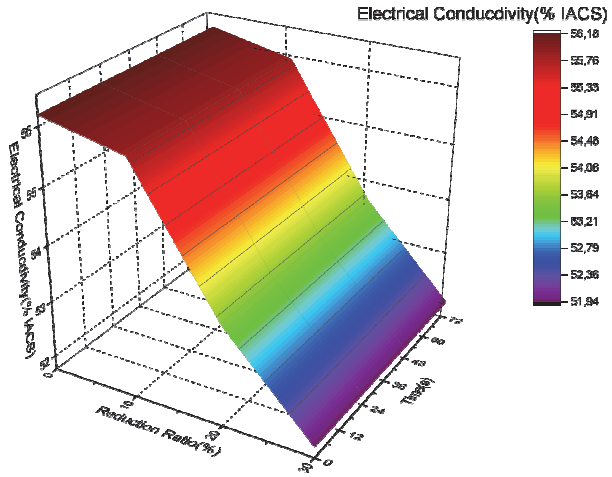

Figure 14 Model 3 billet electrical conductivity change after 30% reduction 0, 10%, 20%, 30% reduction

In Fig. 14 and Fig. 15, the electrical conductivity-deformation-time graphs of the Model 3 and Model 4 trimetallic cylindrical parts are shown. Same as can be remembered from single cylindrical billets, copper is the material with the highest electrical conductivity. For this reason, Model 3, which contains copper, has a very high electrical conductivity but lower when compared to model 1. As Model 4 is a brass-containing model, its electrical conductivity is low but higher than Model 2. The aluminium billet in the middle of Model 3 and Model 4 increased the lower electrical conductivity values, but decreased the higher values. Model 3 and Model 4 have 56,18% IACS and 22,28% IACS electrical conductivity, respectively, for 0% deformation amount, that is, before the upsetting process starts. After 30% deformation, these electrical conductivity values decrease to 51,94% and 19,78%, respectively. The loss rate in electrical conductivity after upsetting for Model 3 is 0,075%, for Model 4 it is around 0,112%.

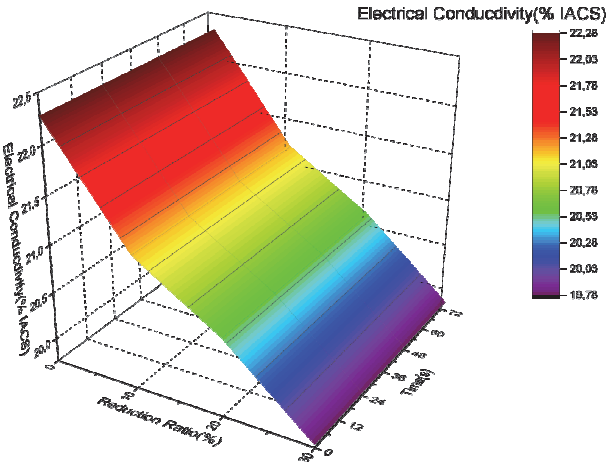

Figure 15 Model 4 billet electrical conductivity change after 30% reduction 0, 10%, 20%, 30% reduction

4 CONCLUSION

In this study, the change and effect of bimetallic and trimetallic materials and the electrical conductivity of single materials forming these materials by upsetting process, which is one of the cold plastic deformation methods, has been investigated experimentally.

The electrical conductivity of both single, bimetallic and trimetallic materials decreases with increasing deformation rate. This reduction amount is different for each material, but 0,025% for copper, 0,0825% for aluminium, 0,0725% for brass and 0,175% for steel, 0,05% for Model 1, 0,2% for Model 2, 0,075% for Model 3, and Model 4 measured at approximately 0,112%.

The decrease rate in electrical conductivity amounts was determined to be lower in materials with high pre-deformation electrical conductivity value, and higher in materials with lower electrical conductivity values. Steel-based and Brass-based materials are more affected by plastic deformation in terms of electrical conductivity than Al and Cu-based materials.

Model 1 and Model 2 bimetallic materials have higher electrical conductivity than Model 3 and Model 4 trimetallic materials and are less affected by cold plastic deformation. Model 1 bimetallic material and Model 3 trimetallic material have high electrical conductivity but low strengths due to the copper material they contain. Model 2 bimetallic and Model 4 trimetallic material were found to have low electrical conductivity but high compressive strength due to the brass material they contain.

Considering the usage areas of bimetallic and trimetallic materials, it is very important to know the relationships between their electrical conductivity and deformation mechanisms. This study sheds light on the future in terms of the production and material selection of bimetallic and trimetallic materials in the industrial sense. In addition, this research can be expanded by selecting different cold working methods such as ECAP, rolling, extrusion and different material combinations.

5 REFERENCES

[1] Avner, S. H. (1998). *Introduction to Physical Metallurgy*. New York, NY, USA, McGraw Hill Inc.

[2] Çetinarslan, C. S. (2009). Effect of cold plastic deformation on electrical conductivity of various materials. *Materials & Design*, *30*(3), 671-673. https://doi.org/10.1016/j.matdes.2008.05.035

[3] Lu, D.-P., Wang, J., Zeng, W.-J., Liu, Y., Lu, L., & Sun, B.-D. (2006). Study on high-strength and high-conductivity Cu-Fe-P alloys. *Materials Science and Engineering: A*, *421*(1), 254-259. https://doi.org/10.1016/j.msea.2006.01.068

[4] Rontó, V., Nagy, E., Svéda, M., Tomolya, K., Varga, F., & Molnár, B. (2007). Developing Mechanical Properties and Electrical Conductivity of Cu Alloys by Jominy End-Quench Test. *Materials Science Forum*, 537-538, 55-62. https://doi.org/10.4028/www.scientific.net/MSF.537-538.55

[5] Plančak, M., Car, Z., Kršulja, M., Vilotić, D., Kačmarcik, I., & Movrin, D. (2012). Possibilities to Measure Contact Friction in Bulk Metal Forming. *Tehnicki Vjesnik - Technical Gazette*, *19*(4), 727-734.

[6] Qi, Y., Lapovok, R., & Estrin, Y. (2016). Microstructure and electrical conductivity of aluminium/steel bimetallic rods processed by severe plastic deformation. *Journal of Materials Science*, *51*(14), 6860-6875. https://doi.org/10.1007/s10853-016-9973-9

[7] Wei, K. X., Wei, W., Wang, F., Du, Q. B., Alexandrov, I. V., & Hu, J. (2011). Microstructure, mechanical properties and electrical conductivity of industrial Cu-0.5%Cr alloy processed by severe plastic deformation. *Materials Science and Engineering A*, *528*(3), 1478-1484. https://doi.org/10.1016/j.msea.2010.10.059

[8] Slany, M., Sedlak, J., Zouhar, J., Zemcik, O., Chladil, J., Jaros, A., Kouril, K., Varhanik, M., Majerik, J., Barenyi, I., & Cep, R. (2021). Material and Dimensional Analysis of Bimetallic Pipe Bend with Defined Bending Radii. *Tehnicki Vjesnik - Technical Gazette*, *28*(3), 974-983. https://doi.org/10.17559/TV-20200409093723

[9] Mróz, S., Szota, P., Dyja, H., & Kawałek, A. (2011). Theoretical and experimental analysis of the Cu-Al bimetallic bar rolling process. *Metalurgija*, *50*(2), 85-88.

[10] Ayer, Ö. (2017). A numerical study for prediction of forming load and experimental verification of bimetallic disc upsetting. *Tehnicki Vjesnik - Technical Gazette*, *24*(6), 1679-1688. https://doi.org/10.17559/TV-20160130154750

[11] Essa, K., Kacmarcik, I., Hartley, P., Plancak, M., & Vilotic, D. (2012). Upsetting of bi-metallic ring billets. *Journal of Materials Processing Technology*, *212*(4), 817-824. https://doi.org/10.1016/j.jmatprotec.2011.11.005

[12] Cetintav, I (2014). *Investigation of Mechanical Properties of Bi-metallic Components Produced used Different Materials*. Master's Thesis, Edirne, Trakya University.

[13] Rodrigues, N. F. M. (2016). *Development of a miniaturized electrical conductivity gauge based on eddy currents testing*. Master's Thesis, Lisboa, Tecnico Lisboa.

[14] *Nondestructive Evaluation Techniques : Eddy Current Testing*. Retrieved December 5, 2021, from https://www.nded.org/NDETechniques/EddyCurrent/Instrumentation/impedanceplane.xhtml

Contact information:

Isik CETİNTAV, Research Assistant
Trakya University, Engineering Faculty,
Edirne, Turkey
E-mail: isikcetintav@trakya.edu.tr

Cenk MISIRLI, Associated Professor
(Corresponding author)
Trakya University, Engineering Faculty,
Edirne, Turkey
E-mail: cenkm@trakya.edu.tr

Yilmaz CAN, Professor
Trakya University, Engineering Faculty,
Edirne, Turkey
E-mail: ycan@trakya.edu.tr